2. CAUSES OF THE EXTREME DRY CONDITIONS OVER CALIFORNIA DURING EARLY 2013

Hailan Wang and Siegfried Schubert

Summary. The 2013 SST anomalies produced a predilection for California drought, whereas the long-term warming trend appears to make no appreciable contribution because of the counteraction between its dynamical and thermodynamic effects

Introduction. The state of California experienced extreme dry conditions during early 2013. In particular, January and February received 28% and 15%, respectively, of their normal monthly rainfall. When January and February are combined, January/February 2013 is ranked as the driest of the period 1895–2014. Such large precipitation deficits exerted enormous stress on water resources in an already high water-demand region. Thus, it is of practical importance to investigate the causes of this extreme climate event so as to assess its predictability.

Climatologically, the winter precipitation over California comes from North Pacific storms that travel eastward under the guidance of the strong North Pacific jet stream. The oceanic storms transport abundant water vapor inland, with heavy precipitation occurring as the flow encounters the Sierra Nevada mountain range. Given the geographical location of California, likely factors that affect the year-to-year variations of precipitation there include atmospheric internal variability, the Madden–Julian Oscillation, El Niño–Southern Oscillation, decadal-to-multidecadal oscillations, and long-term climate change. This study investigates the specific physical processes that led to the early 2013 California drought.

Data and Methods. This study makes use of various observations, the NASA Modern Era Retrospective-Analysis for Research and Applications (MERRA; Rienecker et al. 2011), and an ensemble of long-term Atmospheric Model Intercomparison Project (AMIP) model simulations performed with the NASA Goddard Earth Observing System Model, Version 5 Atmospheric General Circulation Model (GEOS-5 AGCM; Rienecker et al. 2008; Molod et al. 2012). The observations include HadISST data (Rayner et al. 2003), Global Precipitation Climatology Project (GPCP) precipitation (Adler et al. 2003), and Global Precipitation Climatology Centre (CPCC) land precipitation (Schneider et al. 2014). The GEOS-5 AMIP simulations consist of 12 ensemble members, forced with observed monthly SST, sea ice, and time-varying greenhouse gases for the period 1871–present (Schubert et al. 2014). The model was run with 72 hybrid-sigma vertical levels extending to 0.01 hPa and with 1° horizontal resolution on a latitude/longitude grid.

Since the extreme precipitation deficit over California during early 2013 mainly occurred during January and February, our analysis focuses on the average of these two months.

Results. a. Effects of SST and atmospheric internal variability. Figure 2.1 portrays the early 2013 California drought in the context of current climate (1980–2013). Figure 2.1a shows that the observed January–February averaged precipitation deficits over northern California are essentially the land extension of a broad precipitation deficit centered over the northeast Pacific. An examination of daily precipitation and atmospheric circulation fields (not shown) reveals that the California precipitation deficit is the result of a substantial reduction in North Pacific storms reaching the West Coast of the United States, due to the blocking by persistent upper-level high pressure anomalies over the northeast Pacific (Fig. 2.1b). Such a high pressure anomaly over the northeast Pacific is rather typical of dry winters over California (Fig. 2.1c). The underlying causes of the high anomaly, however, appear to vary from winter to winter.

To investigate the physical processes for the early 2013 dry event, we turn to the GEOS-5 AMIP simulations. The AMIP ensemble average highlights the forced signals, primarily those by SST anomalies, whereas the spread among the ensemble members reflects the unforced variability or noise generated by processes internal to the atmosphere. The largest SST anomalies during this time occur mainly in the North Pacific, with a warm anomaly in the central North Pacific and cold anomalies to its west and east (Fig. 2.1f). The tropical SST anomalies are weak overall, with indications of warming over the western tropical Pacific and cooling along the central and

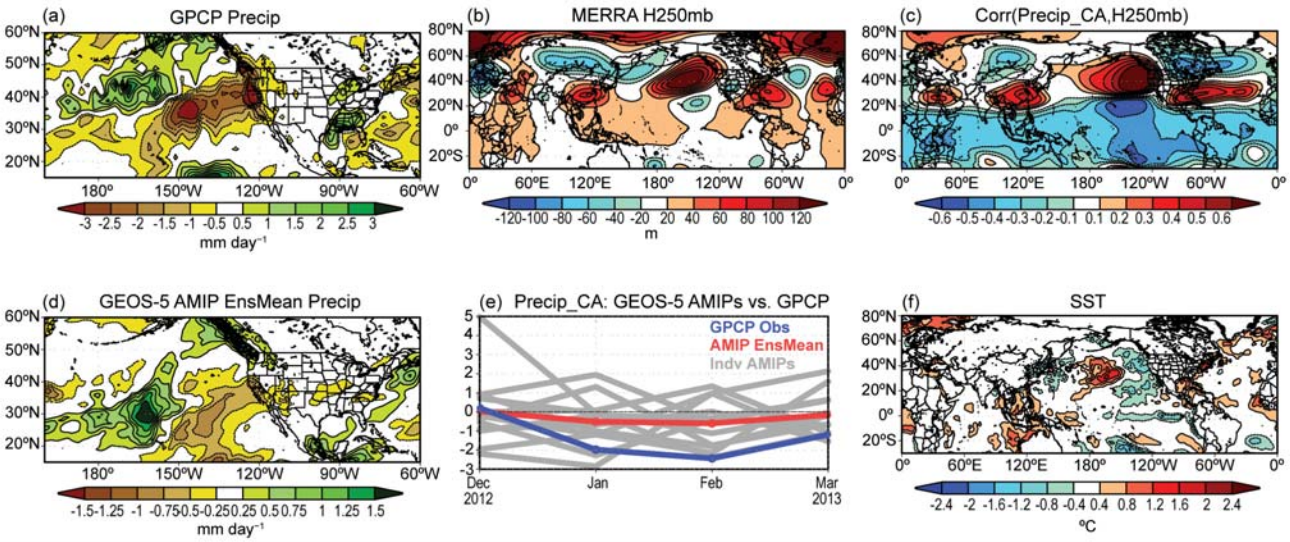

Fig. 2.1. (a) The observed precipitation anomalies (mm day^{-1}) for Jan/Feb 2013 from GPCP. (b) The observed 250-mb geopotential height anomalies (in meters) for Jan/Feb 2013 from MERRA. (c) The temporal correlation between MERRA 250-mb geopotential height and GPCP precipitation averaged over California for Jan/Feb of 1980–2013. A linear trend was removed for each calendar month before computing the correlation. The sign of the correlation is reversed to correspond to precipitation deficit conditions over California. (d) The NASA GEOS-5 AMIP ensemble mean simulation of precipitation anomalies (mm day^{-1}) for Jan/Feb 2013. (e) The comparison between the GPCP (blue), the 12 GEOS-5 AMIP members (gray), and their ensemble mean (red) for monthly precipitation anomalies (mm day^{-1}) averaged over California for Dec 2012–Mar 2013. (f) The observed SST anomalies (°C) for Jan/Feb 2013. The above anomalies are obtained as deviations from their climatology over the period 1980–2013.

eastern equatorial Pacific. When forced with the observed SST anomalies, the GEOS-5 AGCM produces a reasonably good simulation of the observed precipitation anomalies over the North Pacific and western North America. While considerably weaker than observed, the ensemble mean, nevertheless, reproduces the basic pattern of a dry response over California as the land extension of a broad oceanic precipitation decrease over the northeast Pacific (Fig. 2.1d). Figure 2.1e further compares the observed monthly precipitation anomalies averaged over California with each of the 12 ensemble members as well as the 12-member ensemble mean. The observations generally fall within the ensemble spread of the 12 members, though they are clearly on the dry edge of the model spread. The ensemble spread is large, with 2 members showing wet anomalies and 10 members producing dry anomalies over California during early 2013, resulting in a weak negative anomaly in the mean. The above results suggest that while the observed SST anomalies have produced a predilection for dryness over California, the large magnitude of the event is primarily an unforced component of the atmospheric internal variability.

b. Role of long-term warming trend. To investigate any long-term changes in the occurrence of extreme dry events over California, we compare two periods: 1871–1970 and 1980–2013. The latter is marked by a period of enhanced global warming. These two periods are chosen because they remove most of the effects of any phase changes of decadal to multidecadal oscillations such as the Pacific Decadal Oscillation (PDO) and Atlantic Multidecadal Oscillation (AMO); their contrast, thus, highlights the effect of the long-term warming trend. This is verified in Fig. 2.2a, in which the January/February mean SST differences between the two periods show warming over most of the global ocean, with little indications of PDO and AMO. The differences strongly resemble the global SST trend pattern that is obtained as the leading rotated empirical orthogonal function (REOF) pattern of annual mean SST over the 20th century (Schubert et al. 2009), further supporting that they essentially reflect the long-term warming trend. The change of mean upper-level geopotential height from the early period to the current period (Fig. 2.2b) shows generally positive values, with the main centers of the increase occurring over the North Pacific and eastern United States. The Pacific jet stream also weakens considerably, particularly in the jet exit region at 32°N (not shown). We note that such atmospheric circulation changes resemble the responses of this model and four other AGCMs participating in the U.S. Climate Variability and Predictability Program

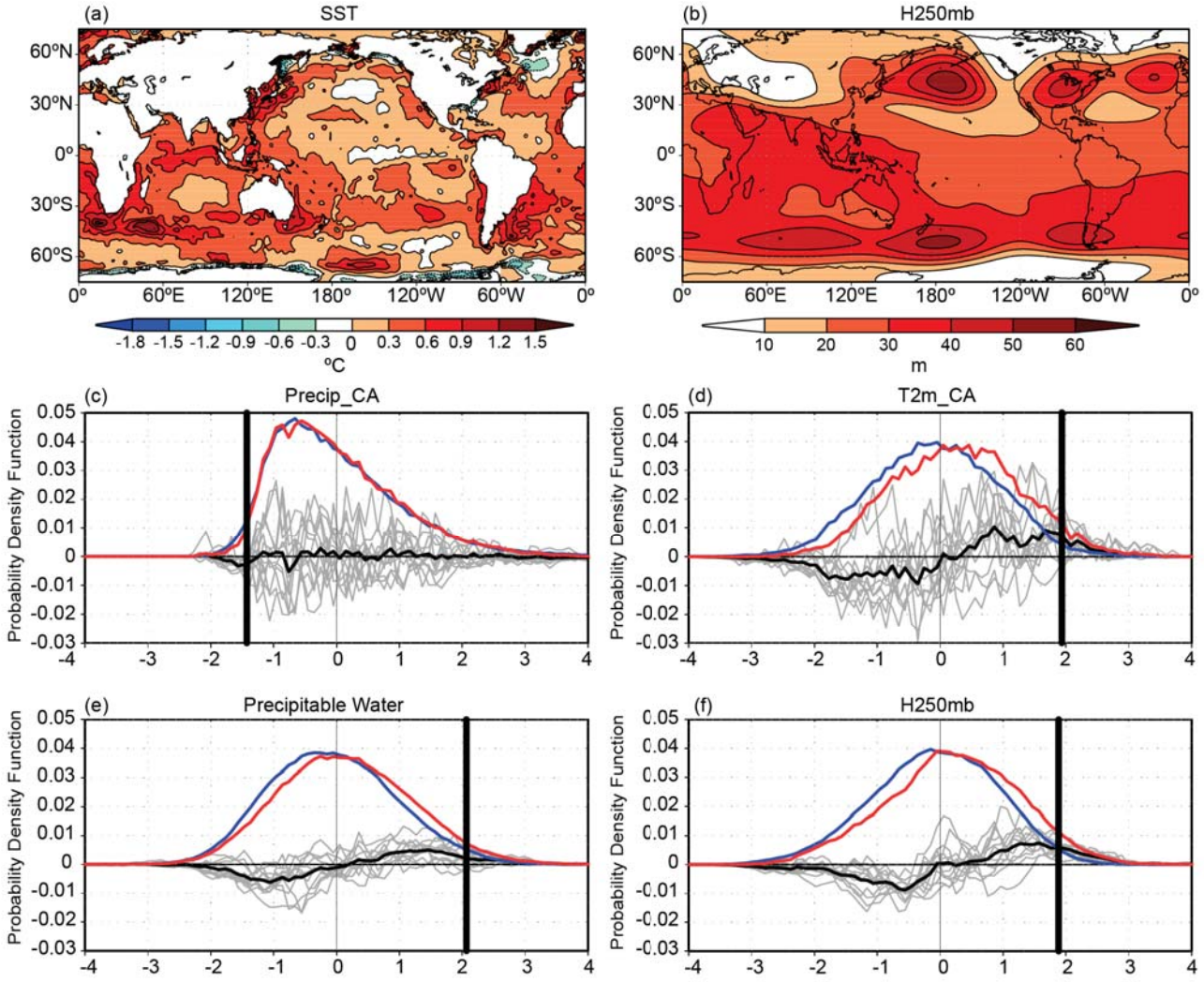

Fig. 2.2. (a) The observed climatology difference of January/February SST (°C) between the period 1871–1970 and the period 1980–2013. (b) Same as (a) but for the 250-mb geopotential height (in meters) in the GEOS-5 AMIP ensemble mean simulation. (c) The PDF of precipitation over California for the period 1871–1970 (blue) and for the period 1980–2013 (red) using the 12 GEOS-5 AMIP simulations, the PDF difference between the two time periods using the 12 AMIP simulations (black), and each of the 12 AMIP simulations (gray). (d) Same as (c) but for surface air temperature over California. (e) same as (c) but for total column water vapor over the northeast Pacific just off the west coast of California (205°–242°E; 25°–42°N). (f) Same as (c) but for the 250-mb geopotential height over the northeast Pacific (205°–240°E; 30°–54°N)—the region that has the peak correlation in Fig. 2.1c, where the upper-level ridge anomalies exert the strongest dry impact over California. The PDF analysis in (c)–(f) uses data at all grid points in the selected domains. Anomalies used in the PDF analysis are deviations from the climatology over the period 1871–2013. The critical values of 2.5% associated with dryness over California based on the PDF distribution over 1871–2013 are shown using thick black vertical lines.

drought working group (Schubert et al. 2009) to the above-mentioned warm trend pattern, suggesting such circulation changes are indeed a robust response to the warming trend pattern. The implication of the above mean circulation changes is that the weaker westerlies may reduce the number of North Pacific storms reaching California and thereby enhance the risk of dry events over California.

To quantify the effect of the long-term warming trend on the occurrence of dry winters over California, we examine the changes in the probability distribution function (PDF) of the January/February mean precipitation between the early and current periods, again based on the 12 GEOS-5 AMIP simulations. Figure 2.2c shows that the PDF of precipitation over California shows no notable change, consistent with a similar PDF analysis using the GPCC precipitation observations (not shown). We note that, for both the GEOS-5 AMIP simulations and the GPCC observations, the mean precipitation over California does not show any noticeable changes between the two periods either. This suggests that there was no increased risk

of drought in California during 2013 as a result of the long-term warming trend. Nevertheless, there are clear indications of an increased probability of warmer surface air temperature over California (Fig. 2.2d), a moister atmosphere over the northeast Pacific off the west coast of California (Fig. 2.2e), and increased height anomalies over the northeast Pacific (Fig. 2.2f)—consistent with the mean height differences found over the North Pacific (Fig. 2.2b). The weakened westerlies on the southern flank of the enhanced northeast Pacific ridge reduces the number of North Pacific storms reaching California thereby increasing the chances of dryness over California, whereas the more abundant atmospheric water vapor off the west coast of California enhances the water vapor transport inland and would likely increase the wetness over California. It thus appears that the effects of the above dynamical and thermodynamic processes counteracted each other, contributing to no appreciable change in the PDF of precipitation over California for these two periods. Therefore, dry climate extremes over California, such as the dry event during early 2013, are unlikely influenced appreciably by the long-term warming trend since the late 19th century.

Conclusions. The extreme precipitation deficits over California during early 2013 resulted from considerably less North Pacific storms reaching California, due to the blocking by persistent high anomalies over the northeast Pacific. Our model results show that the concurrent SST anomalies do force a predilection for dry events over California though considerably weaker than observed, suggesting that atmospheric internal variability accounts for the extreme magnitude of this climate event. An assessment of the role of the long-term warming trend shows that it forces a high anomaly over the northeast Pacific resulting in less North Pacific storms reaching California. The warming trend, however, also leads to increased atmospheric humidity over the northeast Pacific, thus, facilitating wetter events over California. The above two effects appear to counteract each other, contributing to no appreciable long-term change in the risk for dry climate extremes over California since the late 19th century.